

# Probing New Physics with Pulsar Timing Arrays

Zu-Cheng Chen (陈祖成)

Done with Yan-Chen Bi, Qing-Guo Huang, Jun Li, Lang Liu, Zhu Yi,  
Chen Yuan, You Wu, Yu-Mei Wu

Based on 1906.11549 (PRD Rapid Communications); 1910.12239 (PRL);  
2307.01102 (PRDL); 2307.14911 (JCAP); 2310.16500 (JCAP);  
2310.08366 (PRDL); 2401.09818 (PRDL); 2101.06869 (SCPMA);  
2108.10518 (ApJ); 2109.00296 (CTP); 2310.11238 (PRD)  
2302.00229 (PRD); 2310.07469 (CQG)

湖南师范大学

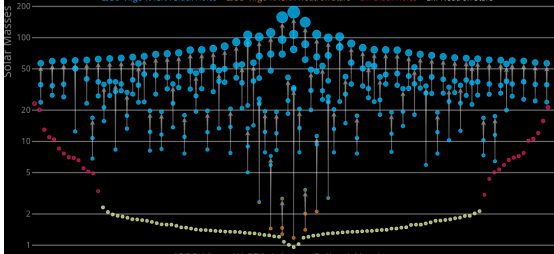
2024-06-03 © 海南大学物理与光电工程学院



海南大学  
HAINAN UNIVERSITY

## Masses in the Stellar Graveyard

LIGO-Virgo-KAGRA Black Holes   LIGO-Virgo-KAGRA Neutron Stars   EM Black Holes   EM Neutron Stars



# The Nobel Prize in Physics 2017



© Nobel Media. III. N  
Elmehed  
**Rainer Weiss**  
Prize share: 1/2

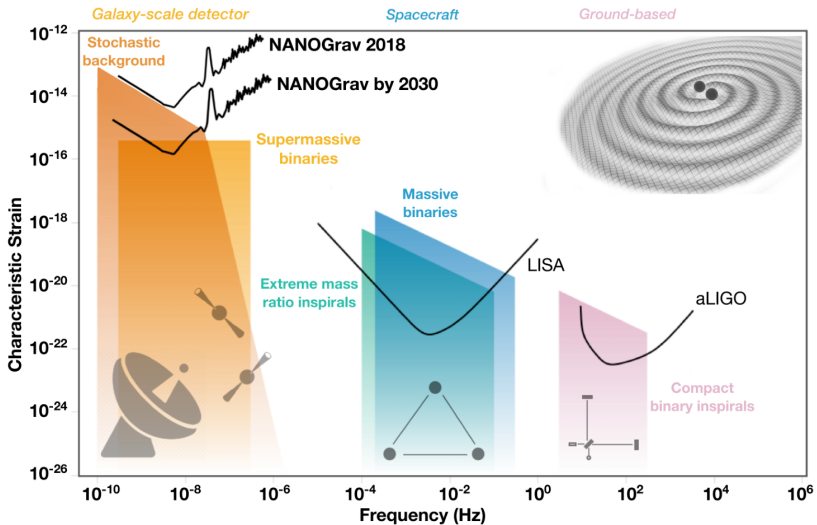


© Nobel Media. III.  
Elmehed  
Barry C. Barish  
Prize share: 1/4

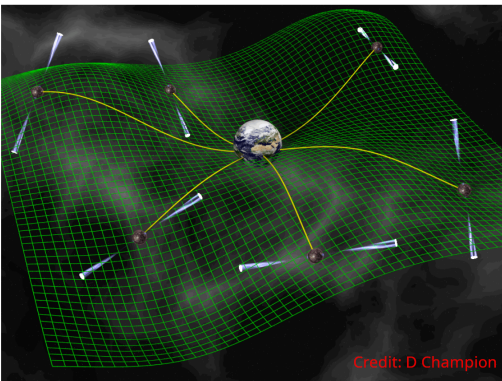
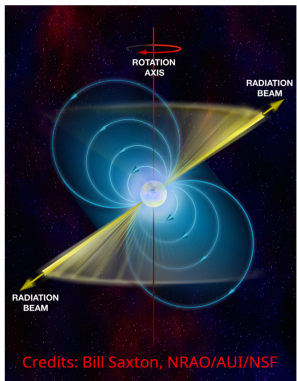


© Nobel Media. III.  
Elmehed  
**Kip S. Thorne**  
Prize share: 1/4

- New era of GW astronomy
  - Multi-messenger astronomy



# Pulsar and pulsar timing array (PTA)



- Pulsars are highly magnetized, rotating neutron stars that emit regular pulses of electromagnetic radiation.
- GWs can cause tiny distortion in spacetime inducing variations in the time of arrivals (ToAs).
- A PTA pursues to detect nHz GWs by regularly monitoring ToAs from an array of the ultra rotational stable millisecond pulsars.

## PTAs in operation



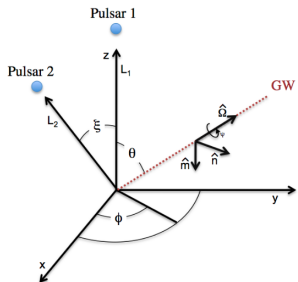
IPTA: PPTA + EPTA + NANOGrav + InPTA

Observers: CPTA, MPTA

## Timing residual induced by a GWB

- Redshift

$$\begin{aligned} z(t, \hat{\Omega}) &= \frac{\nu_e - \nu_p}{\nu_p} \\ &= \frac{\hat{p}^i \hat{p}^j}{2(1 + \hat{\Omega} \cdot \hat{p})} \left[ h_{ij} \left( t_p, \hat{\Omega} \right) - h_{ij} \left( t_e, \hat{\Omega} \right) \right] \\ z(t) &= \int_{S^2} d\hat{\Omega} z(t, \hat{\Omega}) \end{aligned}$$



- Timing residual in frequency-domain

$$\tilde{r}(f, \hat{\Omega}) = \frac{1}{2\pi i f} \left( 1 - e^{-2\pi i f L(1 + \hat{\Omega} \cdot \hat{p})} \right) \times \sum_A h_A(f, \hat{\Omega}) F^A(\hat{\Omega})$$

- Antenna pattern

$$F^A(\hat{\Omega}) = e_{ij}^A(\hat{\Omega}) \frac{\hat{p}^i \hat{p}^j}{2(1 + \hat{\Omega} \cdot \hat{p})}$$

# Detecting a GWB with PTA

- Assume the GWB is isotropic, unpolarized, and stationary

$$\left\langle h_A^*(f, \hat{\Omega}) h_{A'}(f', \hat{\Omega}') \right\rangle = \frac{3H_0^2}{32\pi^3 f^3} \delta^2(\hat{\Omega}, \hat{\Omega}') \delta_{AA'} \delta(f - f') \Omega_{\text{gw}}(f)$$

- Spectrum of GWB

$$\Omega_{\text{gw}}(f) \equiv \frac{1}{\rho_{\text{crit}}} \frac{d\rho_{\text{gw}}}{d \ln f}, \quad \rho_{\text{crit}} = \frac{3H_0^2}{8\pi}, \quad \rho_{\text{gw}} = \frac{1}{32\pi} \left\langle \dot{h}_{ij}(t, \vec{x}) \dot{h}^{ij}(t, \vec{x}) \right\rangle,$$

- Cross-power spectral density

$$S_{IJ} = \left\langle \tilde{r}_I^*(f) \tilde{r}_J(f') \right\rangle = \frac{1}{\gamma} \frac{H_0^2}{16\pi^4 f^5} \delta(f - f') \Gamma_{IJ}(f, L_I, L_J, \xi) \Omega_{\text{gw}}(f)$$

- Overlap reduction function (ORF) is function of  $f, L_I, L_J, \xi$

$$\Gamma_{IJ} = \gamma \sum_A \int d\hat{\Omega} \left( e^{2\pi i f L_I (1 + \hat{\Omega} \cdot \hat{p}_I)} - 1 \right) \times \left( e^{-2\pi i f L_J (1 + \hat{\Omega} \cdot \hat{p}_J)} - 1 \right) F_I^A(\hat{\Omega}) F_J^A(\hat{\Omega})$$

- Hellings & Downs correlations for  $fL \gg 1$  (short-wavelength approximation)

$$\Gamma_{IJ} = \frac{3}{2} \left( \frac{1 - \cos \xi}{2} \right) \ln \frac{1 - \cos \xi}{2} - \frac{1 - \cos \xi}{8} + \frac{1}{2}$$

# Time of arrivals (TOAs)

$$\tau = \tau^{\text{TM}} + n = \tau^{\text{TM}} + \tau^{\text{RN}} + \tau^{\text{DM}} + \tau^{\text{WN}} + \tau^{\text{GW}}$$

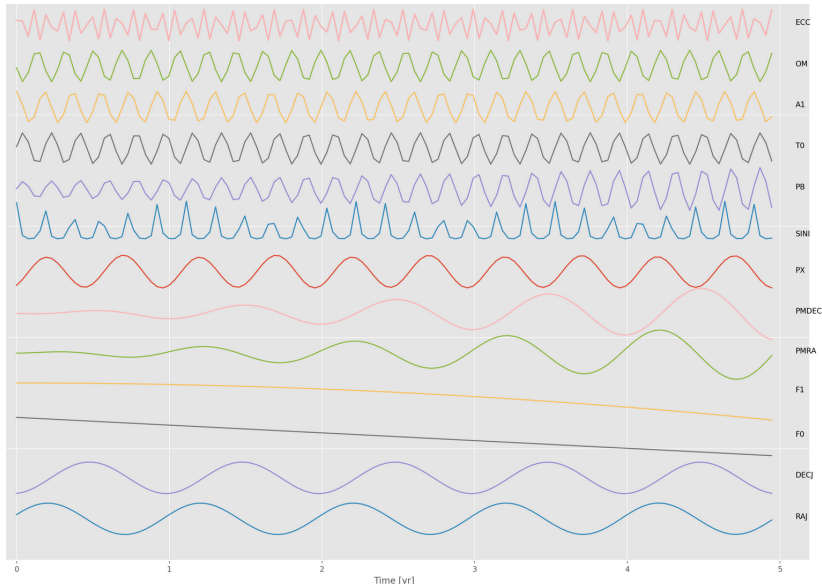
- $\tau^{\text{TM}}$  – timing model: physical model for TOAs taking in to account spin period, proper motion, binary orbital dynamics, etc.
- $\tau^{\text{RN}}$  – red noise (i.e. low-frequency correlated noise). Correlation timescales on the order of weeks - years
- $\tau^{\text{DM}}$ : Model for time-varying dispersion measure variations (i.e. has  $1/\nu^2$  dependence, where  $\nu$  is the radio frequency)
- $\tau^{\text{WN}}$  – white noise: it is more than just a variance since we have data taken from different observing systems and different telescopes.
- $\tau^{\text{GW}}$  – GW signal

# Timing residuals

$$\begin{aligned}\delta\tau &= \tau^{\text{obs}} - \tau^{\text{det}}(\xi_{\text{est}}) \\&= \tau^{\text{det}}(\xi_{\text{true}}) - \tau^{\text{det}}(\xi_{\text{est}}) + n \\&= \tau^{\text{det}}(\xi_{\text{est}} + \epsilon) - \tau^{\text{det}}(\xi_{\text{est}}) + n \\&= \tau^{\text{det}}(\xi_{\text{est}}) + \frac{\partial \tau^{\text{det}}(\xi_{\text{est}} + \epsilon)}{\partial \xi} \Big|_{\epsilon=0} \epsilon - \tau^{\text{det}}(\xi_{\text{est}}) + n + \mathcal{O}(\epsilon^2) \quad (1) \\&\approx \frac{\partial \tau^{\text{det}}(\xi_{\text{est}} + \epsilon)}{\partial \xi} \Big|_{\epsilon=0} \epsilon + n \\&= M\epsilon + n,\end{aligned}$$

- $M$  is the design matrix and  $\epsilon$  is an offset parameter.
- $\tau^{\text{TM}} \sim \text{milliseconds}$
- $n \sim \text{nano- or microseconds}$

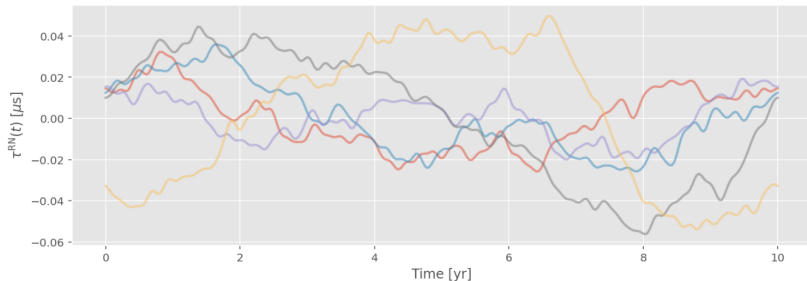
# Timing model



## Red noise

$$\tau_{\text{RN}} = \sum_{j=1}^{N_{\text{mode}}} \left[ a_j \sin \left( \frac{2\pi j t}{T} \right) + b_j \cos \left( \frac{2\pi j t}{T} \right) \right] = F_{\text{red}} a_{\text{red}},$$

- $a_{\text{red}}$  is a vector of the alternating sine and cosine amplitudes
- $T$  is the total time span of the data
- $F_{\text{red}}$  is a  $N_{\text{TOA}} \times 2N_{\text{mode}}$  matrix with alternating sine and cosine terms
- $N_{\text{mode}}$  the number of frequencies used. Typically we use 50 Fourier modes.



# Red noise

- covariance matrix

$$\begin{aligned} K_{\text{red}} &= \langle \tau^{\text{RN}} (\tau^{\text{RN}})^T \rangle \\ &= F_{\text{red}} \langle a_{\text{red}} a_{\text{red}}^T \rangle F_{\text{red}}^T \\ &= F_{\text{red}} \varphi F_{\text{red}}^T \end{aligned}$$

- $\varphi = \langle a_{\text{red}} a_{\text{red}}^T \rangle$  is a matrix with zero off-diagonal elements

$$\varphi_{i,i} = P(f_i)$$

- Power spectrum

- power-law

$$P_{\text{PL}}(f; A, \gamma) = \frac{A^2}{12\pi^2} \left( \frac{f}{\text{yr}^{-1}} \right)^{-\gamma} \text{yr}^3$$

- broken power-law

$$P_{\text{BPL}}(f; A, \gamma, \delta, f_b, \kappa) = \frac{A^2}{12\pi^2} \left( \frac{f}{\text{yr}^{-1}} \right)^{-\gamma} \left( 1 + \left( \frac{f}{f_b} \right)^{1/\kappa} \right)^{\kappa(\gamma-\delta)} \text{yr}^3$$

- free spectrum

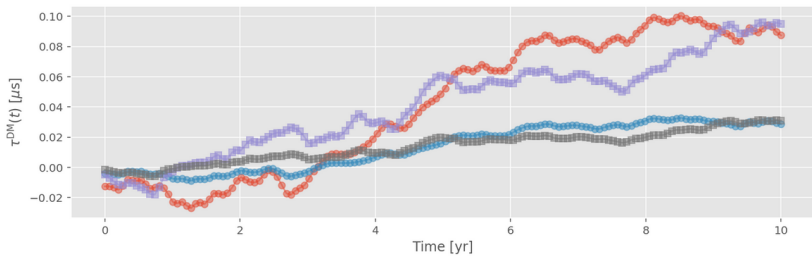
$$P_{\text{FS}}(f_i; \rho_i) = \rho_i^2 T,$$

$\rho_i$  is the spectral amplitude at frequency  $f_i = i/T$ .

# Dispersion measure variations

Dispersion measure is due to the propagation of radio waves through the charged plasma of the interstellar medium (ISM),

$$\text{DM}(t) = \int_0^{L(t)} n_e(\mathbf{x}) d\ell.$$



# Dispersion measure variations

- timing residual

$$\tau^{\text{DM}} = F_{\text{DM}} a_{\text{DM}}$$

- covariance matrix

$$\begin{aligned} K_{\text{DM}} &= F_{\text{DM}} \langle a_{\text{DM}} a_{\text{DM}}^T \rangle F_{\text{DM}}^T \\ &= F_{\text{DM}} \varphi_{\text{DM}} F_{\text{DM}}^T \end{aligned}$$

- $\varphi_{\text{DM}} = \langle a_{\text{DM}} a_{\text{DM}}^T \rangle$  is a matrix with zero off-diagonal elements

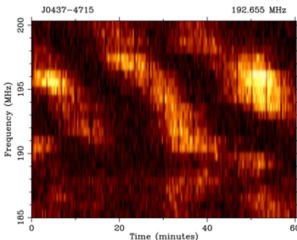
$$\varphi_{i,i} = P(f_i)$$

- radio frequency dependent power spectrum

$$P_{\text{DM}}(f; A_{\text{DM}}, \gamma_{\text{DM}}) = \frac{A_{\text{DM}}^2}{12\pi^2} f_{yr}^{-3} \left( \frac{f}{f_{yr}} \right)^{-\gamma_{\text{DM}}} \left( \frac{1400 \text{MHz}}{\nu} \right)^2$$

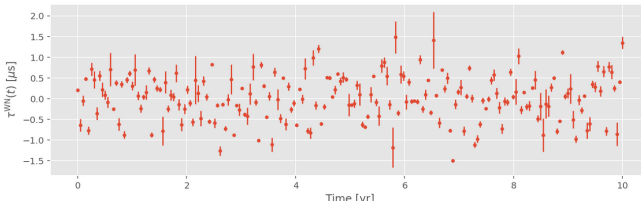
# White noise

- Measurement error is the biggest contributor.
- A function of radio frequencies and observation times.



- covariance matrix

$$N_{ij} = \delta_{ij} \left( \sigma_{\text{meas},ij}^2 + \sigma_{\text{equad},ij}^2 \right),$$



# GWB

$$\tau_{\text{GWB}} = \sum_{j=1}^{N_{\text{mode}}} \left[ a_j \sin\left(\frac{2\pi j t}{T}\right) + b_j \cos\left(\frac{2\pi j t}{T}\right) \right] = F_{\text{GWB}} a_{\text{GWB}},$$

- covariance matrix

$$\begin{aligned} K_{\text{GWB}} &= \langle \tau^{\text{GWB}} (\tau^{\text{GWB}})^T \rangle \\ &= F_{\text{GWB}} \langle a_{\text{GWB}} a_{\text{GWB}}^T \rangle F_{\text{GWB}}^T \\ &= F_{\text{GWB}} \varphi F_{\text{GWB}}^T \end{aligned}$$

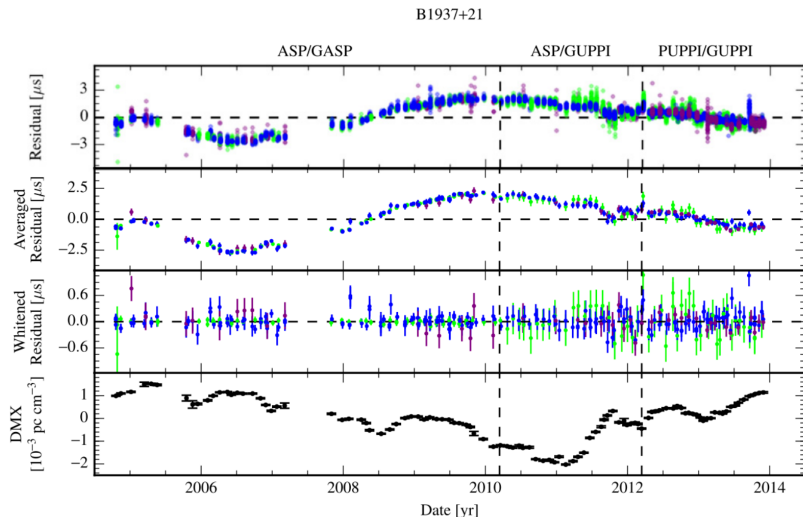
- correlations

$$\varphi_{IJ;i,i} = \Gamma_{I,J} P(f_i)$$

- Power spectrum from SMBHBs

$$P(f; A, \gamma) = \frac{A^2}{12\pi^2} \left( \frac{f}{\text{yr}^{-1}} \right)^{-\gamma} \text{yr}^3$$

# Putting them all together



- timing residuals

$$\begin{aligned}\delta\tau &= M\epsilon + F_{\text{red}}a_{\text{red}} + F_{\text{DM}}a_{\text{DM}} + n \\ &= Tb + n\end{aligned}$$

- definitions

$$T = [M \ F_{\text{red}} \ F_{\text{DM}}]; \quad b = \begin{bmatrix} \epsilon \\ a_{\text{red}} \\ a_{\text{DM}} \end{bmatrix} \quad B = \begin{bmatrix} \infty & & \\ & \varphi & \\ & & \varphi_{\text{DM}} \end{bmatrix}$$

- covariance matrix

$$C = N + K = N + TBT^T$$

where  $N = \langle nn^T \rangle$  is covariance matrix for white noise.

# likelihood

- Basis Picture:

$$p(\delta\tau|b, \phi) = \frac{\exp \left[ -\frac{1}{2}(\delta\tau - Tb)^T N^{-1}(\delta\tau - Tb) \right]}{\sqrt{\det 2\pi N}} \frac{\exp \left[ -\frac{1}{2}b^T B^{-1}b \right]}{\sqrt{\det 2\pi B}}$$

- Kernel Picture

$$p(\delta\tau|\phi) = \frac{\exp \left[ -\frac{1}{2}\delta\tau^T C^{-1}\delta\tau \right]}{\sqrt{\det 2\pi C}}$$

- Woodbury Lemma

$$C^{-1} = (N + TBT^T)^{-1} = N^{-1} - N^{-1}T \left( B^{-1} + T^T N^{-1} T \right)^{-1} T^T N^{-1}$$

$$\det C = \det (N + TBT^T) = \det (N) \det (B) \det (B^{-1} + T^T N^{-1} T)$$

$B \sim 1000 \times 1000$  and  $C \sim 30000 \times 30000$  means speedup of  $\sim 1000$

- Bayes' theorem

$$p(H|D) = \frac{p(D|H)p(H)}{p(D)}$$

↑   ↑  
posterior                                   normalization factor

likelihood                                   prior

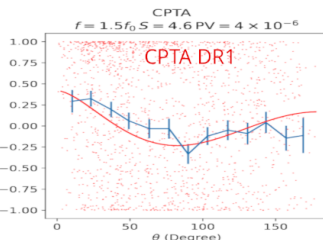
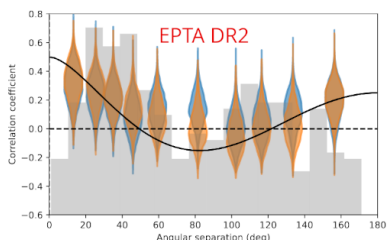
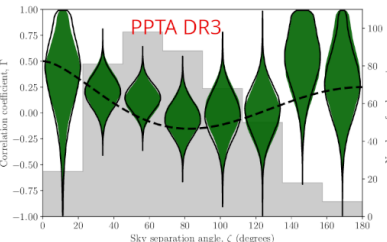
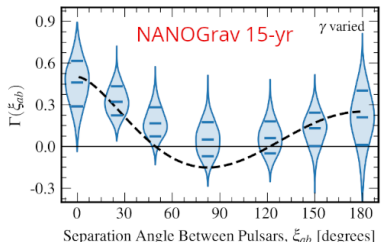
- Bayes factor

$$BF_{12} = \frac{\Pr(\mathcal{D} | \mathcal{H}_1)}{\Pr(\mathcal{D} | \mathcal{H}_2)}$$

**Table 7.1** Evidence categories for the Bayes factor  $BF_{12}$  (Jeffreys, 1961).

Bayes factor $BF_{12}$			Interpretation
	>	100	Extreme evidence for $\mathcal{M}_1$
30	—	100	Very strong evidence for $\mathcal{M}_1$
10	—	30	Strong evidence for $\mathcal{M}_1$
3	—	10	Moderate evidence for $\mathcal{M}_1$
1	—	3	Anecdotal evidence for $\mathcal{M}_1$
	1		No evidence
1/3	—	1	Anecdotal evidence for $\mathcal{M}_2$
1/10	—	1/3	Moderate evidence for $\mathcal{M}_2$
1/30	—	1/10	Strong evidence for $\mathcal{M}_2$
1/100	—	1/30	Very strong evidence for $\mathcal{M}_2$
	<	1/100	Extreme evidence for $\mathcal{M}_2$

# The stochastic signal in PTAs (2023-06-29)



NANOGrav, 2306.16213 (ApJL); PPTA, 2306.16215 (ApJL)

EPTA+InPTA, 2306.16214 (A&A); CPTA, 2306.16216 (RAA)

# SIGWs can explain the PTA signal.

9

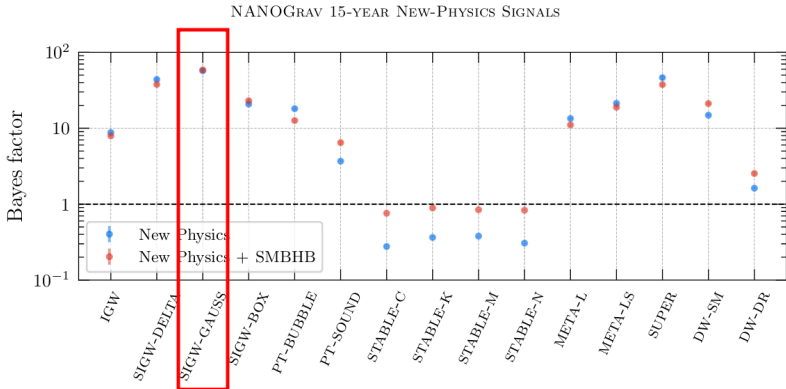


**Figure 2.** Bayes factors for the model comparisons between the new-physics interpretations of the signal considered in this work and the interpretation in terms of SMBHBs alone. Blue points are for the new physics alone, and red points are for the new physics in combination with the SMBHB signal. We also plot the error bars of all Bayes factors, which we obtain following the bootstrapping method outlined in Section 3.2. In most cases, however, these error bars are small and not visible.

NANOGrav Collaboration, 2306.16219 (ApJL)

# Scalar-Induced Gravitational Waves (SIGWs)

- Primordial perturbations can be generated by quantum fluctuations during inflation.
- Metric perturbation in Newtonian gauge

$$ds^2 = a^2 \left\{ -(1 + 2\phi)d\eta^2 + \left[ (1 - 2\phi)\delta_{ij} + \frac{h_{ij}}{2} \right] dx^i dx^j \right\}, \quad (2)$$

where  $\phi \equiv \phi^{(1)}$  and  $h_{ij} \equiv h_{ij}^{(2)}$  are the scalar and tensor perturbations, respectively.

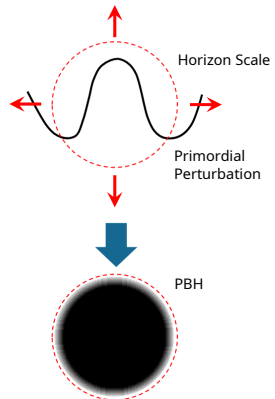
- Primordial scalar perturbation can be the source of SIGWs, as well as primordial black holes (PBHs).

# Primordial black holes (PBHs)

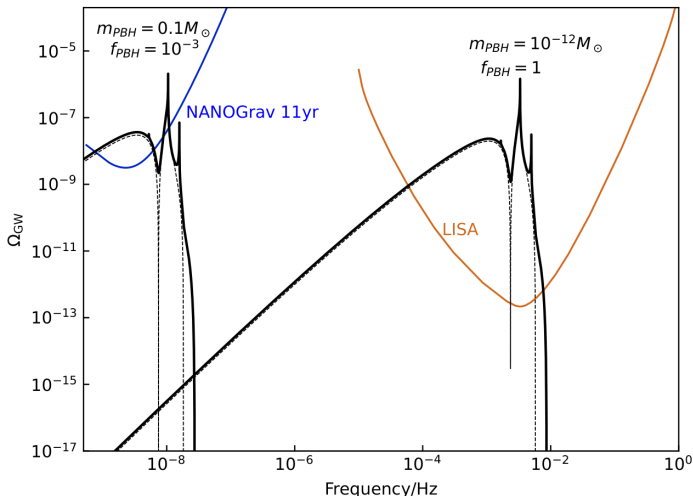
- PBHs are formed in the early universe by gravitational collapse of primordial density perturbations
- PBH mass can span many orders

$$m_{\text{PBH}} \sim \frac{t}{G} \sim 10^{-18} \left( \frac{t}{10^{-23}} \right) M_{\odot} \quad (3)$$

- PBHs survived from Hawking radiation can be DM candidates.
- PBHs can explain LVK BBHs.

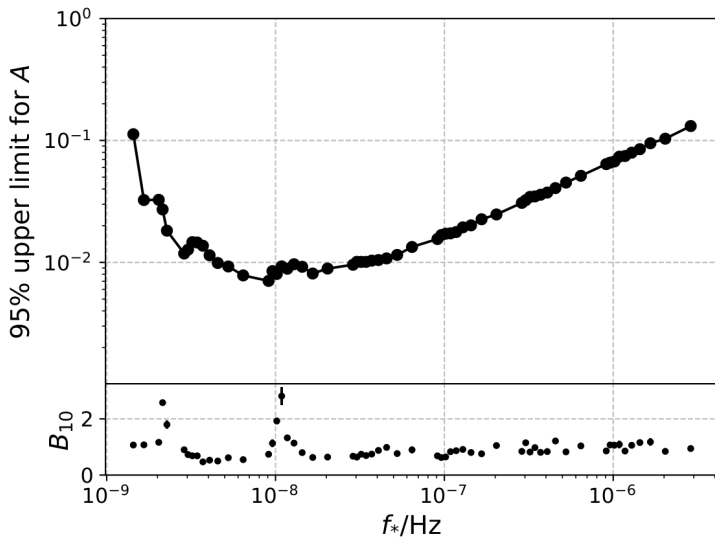


# Detecting SIGW with PTA



Chen Yuan, ZCC, Qing-Guo Huang, 1906.11549 (PRD Rapid Communications)

## Constrain SIGWs with NANOGrav 11-yr data set

*ZCC, Chen Yuan, Qing-Guo Huang, 1910.12239 (PRL)*

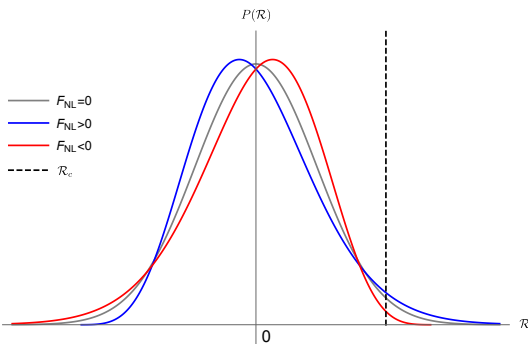
# Non-Gaussianity

- The local-type non-Gaussian curvature perturbations:

$$\mathcal{R}(\vec{x}) = \mathcal{R}_G(\vec{x}) + F_{NL} (\mathcal{R}_G^2(\vec{x}) - \langle \mathcal{R}_G^2(\vec{x}) \rangle). \quad (4)$$

- The effective curvature power spectrum

$$P_{\mathcal{R}}^{\text{NG}} = P_{\mathcal{R}}(k) + F_{NL}^2 \int_0^\infty dv \int_{|1-v|}^{1+v} du \frac{P_{\mathcal{R}}(uk)P_{\mathcal{R}}(vk)}{2u^2v^2}. \quad (5)$$



# Non-Gaussianity

- Power spectrum

$$P_{\mathcal{R}}(k) = \frac{A}{\sqrt{2\pi}\Delta} \exp\left(-\frac{\ln^2(k/k_*)}{2\Delta^2}\right). \quad (6)$$

- The energy density of GWs

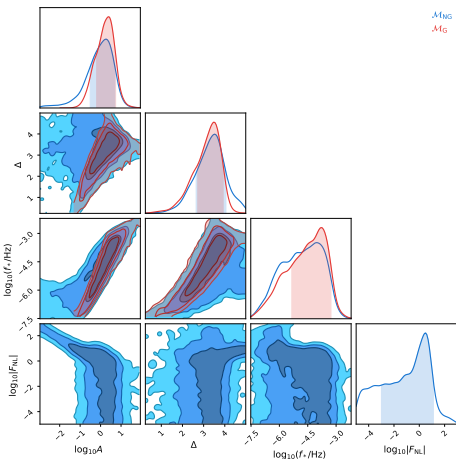
$$\Omega_{\text{GW}}(k) = \int_0^\infty dv \int_{|1-v|}^{|1+v|} du \mathcal{T} P_{\mathcal{R}}^{\text{NG}}(vk) P_{\mathcal{R}}^{\text{NG}}(uk), \quad (7)$$

where the transfer function  $\mathcal{T} = \mathcal{T}(u, v)$  is given by

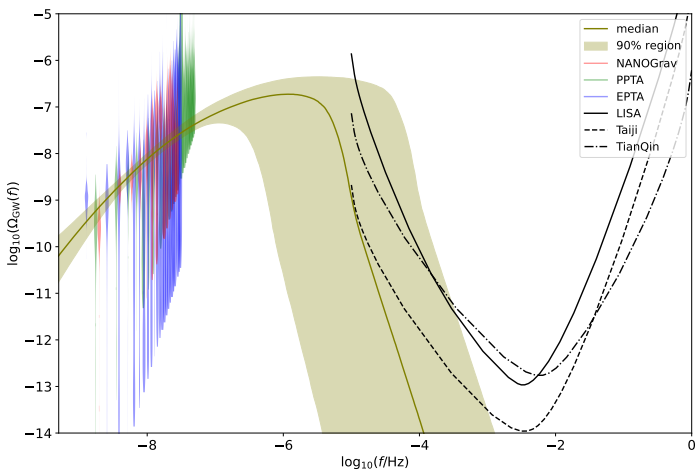
$$\begin{aligned} \mathcal{T}(u, v) = & \frac{3}{1024v^8u^8} \left[ 4v^2 - (v^2 - u^2 + 1)^2 \right]^2 (v^2 + u^2 - 3)^2 \\ & \times \left\{ \left[ (v^2 + u^2 - 3) \ln \left( \left| \frac{3 - (v + u)^2}{3 - (v - u)^2} \right| \right) - 4vu \right]^2 \right. \\ & \left. + \pi^2 (v^2 + u^2 - 3)^2 \Theta(v + u - \sqrt{3}) \right\}. \end{aligned} \quad (8)$$

Rong-gen Cai, Shi Pi, Misao Sasaki, 1810.11000 (PRL)

## PE with NANOGrav 15-yr data set + PPTA DR3 + EPTA DR2



- $|F_{\text{NL}}| \lesssim 13.9$
- $-13.9 \lesssim F_{\text{NL}} \lesssim -0.1$  when further requiring  $f_{\text{PBH}} \lesssim 1$ .



Lang Liu, ZCC, Qing-Guo Huang, 2307.01102 (PRDL)

## Implications

- The constraints on  $F_{\text{NL}}$  have significant implications for multi-field inflation models.
- For instance, adiabatic curvaton models predict that

$$f_{\text{NL}} = \frac{5}{3} F_{\text{NL}} = \frac{5}{4r_D} - \frac{5r_D}{6} - \frac{5}{3}, \quad (9)$$

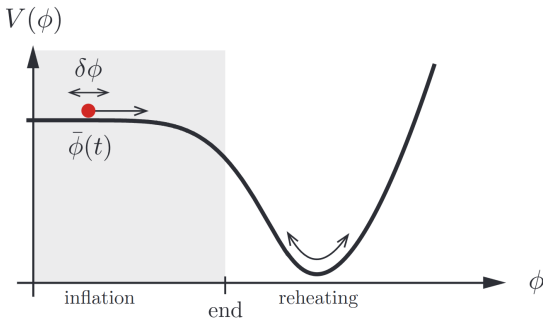
where  $r_D = 3\rho_{\text{curvaton}}/(3\rho_{\text{curvaton}} + 4\rho_{\text{radiation}})$  represents the “curvaton decay fraction” at the time of curvaton decay.

- Our constraint  $-13.9 \lesssim F_{\text{NL}} \lesssim -0.1$  implies

$$r_D \gtrsim 0.62 \quad (95\%), \quad (10)$$

indicating that the curvaton field has a non-negligible energy density when it decays.

# Equation of state of the early Universe

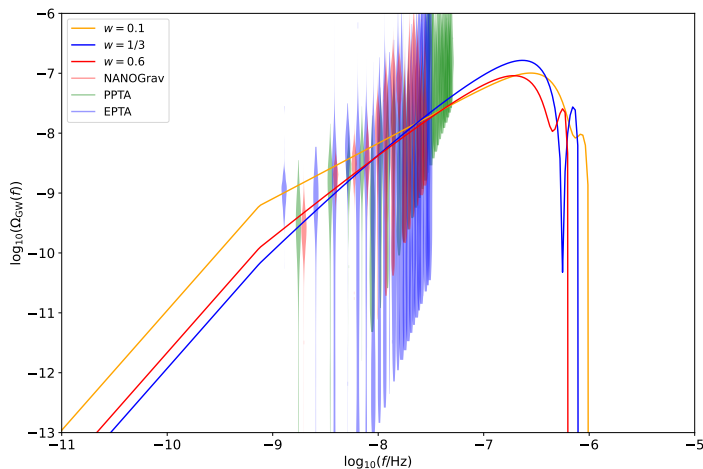


- The SIGW spectrum for the scales  $k \gtrsim k_{\text{rh}}$  is

$$\Omega_{\text{GW},\text{rh}} = \left(\frac{k}{k_{\text{rh}}}\right)^{-2b} \int_0^\infty dv \int_{|1-v|}^{1+v} du \mathcal{T}(u, v, w) \mathcal{P}_{\mathcal{R}}(ku) \mathcal{P}_{\mathcal{R}}(kv), \quad (11)$$

where  $b \equiv (1 - 3w)/(1 + 3w)$ . And  $\Omega_{\text{GW},\text{rh}} \propto (k/k_{\text{rh}})^2$  when  $k \lesssim k_{\text{rh}}$ .

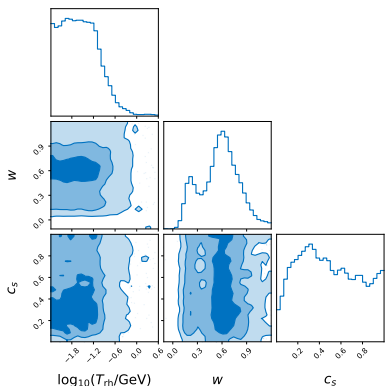
Guillem Domènech, Shi Pi, Misao Sasaki, 2005.12314 (JCAP)



Lang Liu, ZCC, Qing-Guo Huang, 2307.14911 (JCAP)

Lang Liu, You Wu, ZCC, 2310.16500 (JCAP)

## PE with NANOGrav 15-yr data set + PPTA DR3 + EPTA DR2



- Reheating temperature  $T_{\text{rh}} \lesssim 0.2 \text{ GeV}$ .
- $w < 0$  is excluded at 95% CL.
- $w = 1/3$  is consistent with the PTA data.
- $w$  peaks at around 0.6.
- Since during the oscillation of inflaton,  $w = \frac{p-2}{p+2}$  for a potential  $V(\phi) \propto \phi^p$ , then, it implies a  $V(\phi) \propto \phi^8$ .

Lang Liu, ZCC, Qing-Guo Huang, 2307.14911 (JCAP)

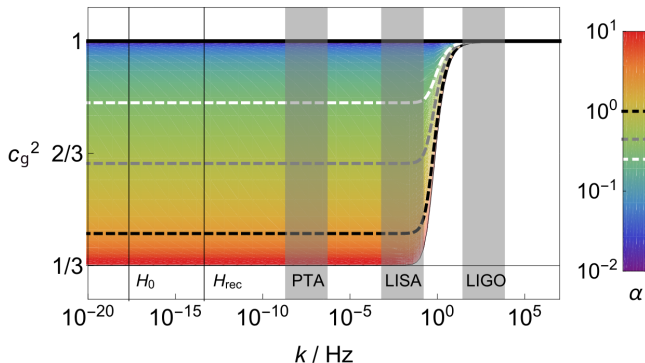
Lang Liu, You Wu, ZCC, 2310.16500 (JCAP)

# Speed of GW

- GW170817:  $-3 \times 10^{-15} \leq c_g - 1 \leq 7 \times 10^{-16}$

LVK, 1710.05832 (PRL)

- $c_g$  can be frequency dependent



Claudia de Rham, Scott Melville, 1806.09417 (PRL)

# Speed of SIGW

- EoM

$$h_{\mathbf{k}}''(\eta) + 2\mathcal{H}h_{\mathbf{k}}'(\eta) + \textcolor{red}{c_g^2}k^2h_{\mathbf{k}}(\eta) = 4S_{\mathbf{k}}(\eta). \quad (12)$$

- SIGW spectrum

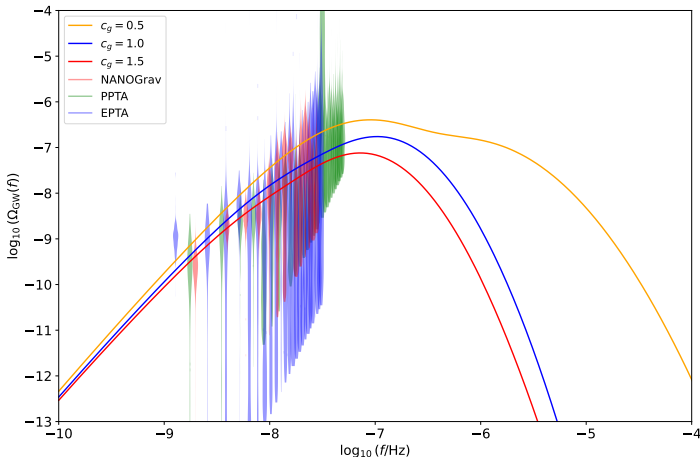
$$\Omega_{\text{GW}}(k) = \int_0^\infty dv \int_{|1-v|}^{1+v} du \mathcal{T}(u, v, \textcolor{red}{c_g}) P_\zeta(vk) P_\zeta(uk). \quad (13)$$

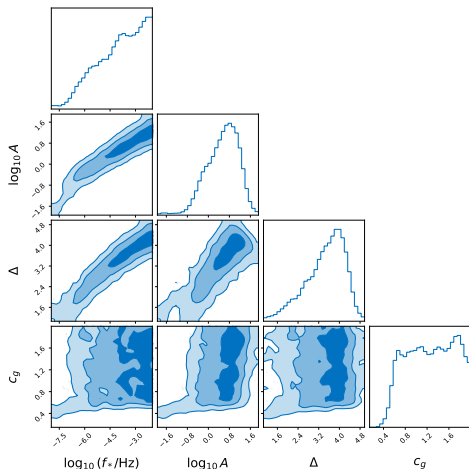
- Transfer function

$$\begin{aligned} \mathcal{T}(u, v, c_g) = & \frac{3 \left[ 4v^2 - (v^2 - u^2 + 1)^2 \right]^2 (v^2 + u^2 - 3c_g^2)^2}{1024v^8u^8} \\ & \times \left\{ \left[ (v^2 + u^2 - 3c_g^2) \ln \left( \left| \frac{3c_g^2 - (v+u)^2}{3c_g^2 - (v-u)^2} \right| \right) - 4vu \right]^2 \right. \\ & \left. + \pi^2 (v^2 + u^2 - 3c_g^2)^2 \Theta(v+u-\sqrt{3}c_g) \right\}. \end{aligned} \quad (14)$$

*Jun Li, Guang-Hai Guo, 2312.04589*

## PE with NANOGrav 15-yr data set + PPTA DR3 + EPTA DR2

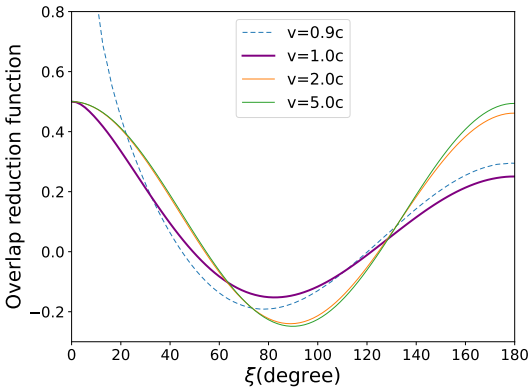




- $c_g \gtrsim 0.61$  at a 95% CI.
- Consistent with  $c_g = 1$ .

ZCC, Jun Li, Lang Liu, Zhu Yi, 2401.09818 (PRDL)

## ORF

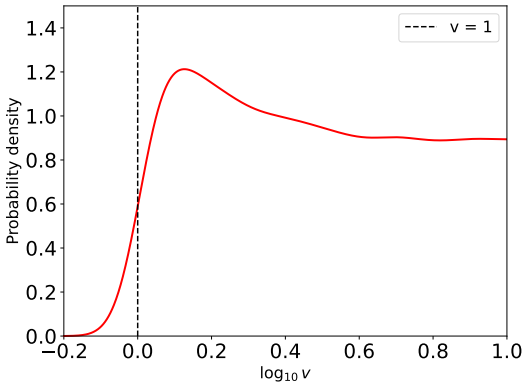


Reginald Christian Bernardo, Kin-Wang Ng, 2208.12538, (PRD)

Reginald Christian Bernardo, Kin-Wang Ng, 2302.11796, (PRDL)

Yan-Chen Bi, Yu-Mei Wu, ZCC, Qing-Guo Huang, 2310.08366 (PRDL)

## PE with NANOGrav 15-yr data set

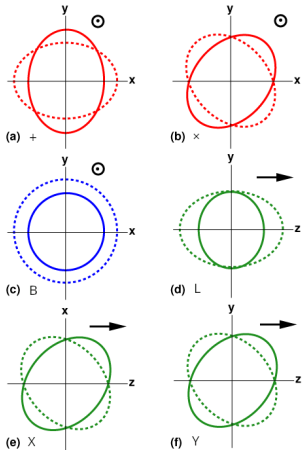


- $c_g \gtrsim 0.85$ .
- Still consistent with  $c_g = 1$ .

Yan-Chen Bi, Yu-Mei Wu, ZCC, Qing-Guo Huang, 2310.08366 (PRDL)

# Alternative Polarizations

## Gravitational-Wave Polarization



- A general metric gravity theory in 4D spacetime can have 6 polarization modes.
- polarization tensors

$$\epsilon_{ij}^+ = \hat{m} \otimes \hat{m} - \hat{n} \otimes \hat{n},$$

$$\epsilon_{ij}^\times = \hat{m} \otimes \hat{n} + \hat{n} \otimes \hat{m},$$

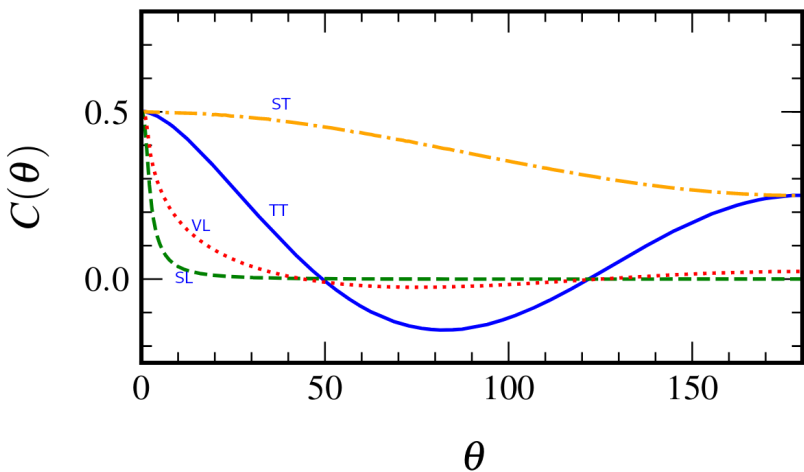
$$\epsilon_{ij}^B = \hat{m} \otimes \hat{m} + \hat{n} \otimes \hat{n},$$

$$\epsilon_{ij}^L = \hat{\Omega} \otimes \hat{\Omega},$$

$$\epsilon_{ij}^X = \hat{m} \otimes \hat{\Omega} + \hat{\Omega} \otimes \hat{m},$$

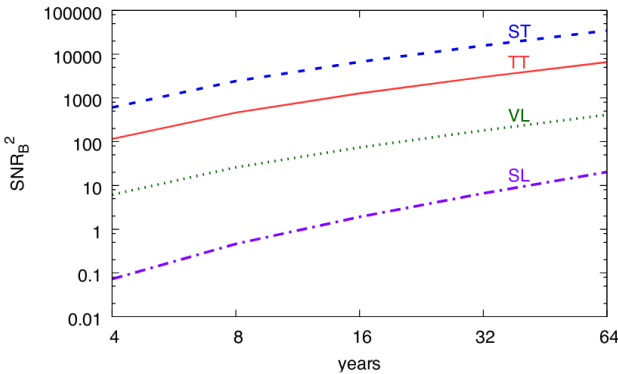
$$\epsilon_{ij}^Y = \hat{n} \otimes \hat{\Omega} + \hat{\Omega} \otimes \hat{n}$$

## ORF



$$|\Gamma_{ST}| > |\Gamma_{TT}| > |\Gamma_{VL}| > |\Gamma_{SL}|$$

$$\text{SNR}_B^2 = 2 \sum_f \sum_a^{N_p} \sum_{b>a}^{N_p} \frac{\Gamma_{ab}^I(f)}{\Gamma_{aa}^I(f)\Gamma_{bb}^I(f) + \Gamma_{ab}^I(f)}.$$



ST is the easiest to detect among the four polarization modes.

Neil J. Cornish, Logan O'Beirne, Stephen R. Taylor, Nicolás Yunes, 1712.07132 (PRL)

# Evidence for the ST correlations in NANOGrav 12.5-yr

- *ZCC, Chen Yuan, Qing-Guo Huang, 2101.06869 (SCPMA)*

	TT	ST	VL	SL	ST+TT
DE438	4.96(9)	107(7)	1.94(3)	0.373(5)	96(3)

- Our results were reproduced  $\sim 8$  months later by *NANOGrav, 2109.14706 (ApJL)*

As shown in Fig. 10, the most favored Bayesian model is a GWB with GW-like monopolar correlations of Eq. (25) with a Bayes factor greater than 100. Additionally, as a cross-check, we have reproduced the results of Chen et al. (2021), where a model with ST correlations with a spectral index of 5, [ST]M3A[5], was compared to a model without correlations and a spectral index of 13/3, M2A[13/3]. We obtain a Bayes factor of

# Search for alternative polarizations in NANOGrav 15-yr data set

- Our paper appeared on arXiv one day prior to NANOGrav's. Both sets of results are broadly consistent with each other.
- *ZCC, Yu-Mei Wu, Yan-Chen Bi, Qing-Guo Huang, 2310.11238 (PRD)*

Model	ST	VL	SL	GTb	TT + ST
BF	0.40(3)	0.12(2)	0.002(1)	3.9(3)	0.943(5)

- *NANOGrav, 2310.12138 (ApJL)*

Our Bayesian analyses show the Bayes factor for HD over ST is  $\sim 2$ , and the Bayes factor for a model with both correlations compared to a model with just HD is  $\sim 1$ . These results are largely consistent with a similar study by Chen et al. (2023), in which they searched NANOGrav's 15 yr data set for nontensorial GWBs on a similar timescale to the work presented here. Taking the spectral parameter recovery into account, as in Figure 3, we found each correlation, when fit for individually, is in agreement with CURN. We also found more informative  $\log_{10} A_g$  and  $\gamma_g$  recovery for HD than ST, and HD parameters show better agreement with CURN spectral parameters when correlations are included together. The analyses in this Letter, as well as those in Bernardo & Ng (2023c) and Chen et al. (2023), do not rule out the possibility of ST correlations in our data. However, our analysis also shows no statistical need for an additional stochastic process with ST correlations.

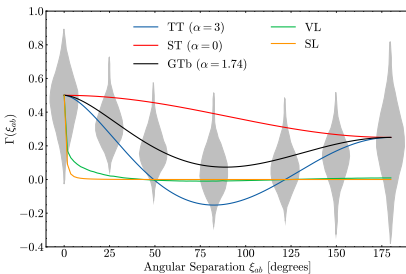
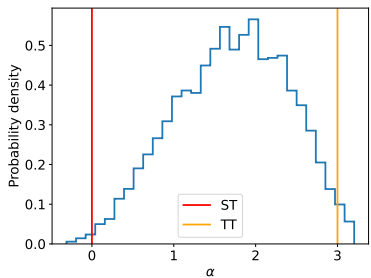
We also consider a parameterized transverse ORF as

$$\Gamma_{ab}(f) = \frac{1}{8} (3 + 4\delta_{ab} + \cos \xi_{ab}) + \frac{\alpha}{2} k_{ab} \ln k_{ab}. \quad (15)$$

ST:  $\alpha = 0$

TT:  $\alpha = 3$

prior of  $\alpha$ : Uniform(-10, 10)



- Our analysis yields  $\alpha = 1.74^{+1.18}_{-1.41}$ , thus excluding both the TT and ST models at the 90% CL.

ZCC, Yu-Mei Wu, Yan-Chen Bi, Qing-Guo Huang, 2310.11238 (PRD)

# Summary

PTAs are promising tools for probing new physics, including:

- SIGW

*Chen Yuan, ZCC, Qing-Guo Huang, 1906.11549 (PRD Rapid Communications)*

*ZCC, Chen Yuan, Qing-Guo Huang, 1910.12239 (PRL)*

- Non-Gaussianity of curvature perturbations

*Lang Liu, ZCC, Qing-Guo Huang, 2307.01102 (PRDL)*

- Equation of state of the early Universe

*Lang Liu, ZCC, Qing-Guo Huang, 2307.14911 (JCAP)*

*Lang Liu, You Wu, ZCC, 2310.16500 (JCAP)*

- Speed of GW

*Yan-Chen Bi, Yu-Mei Wu, ZCC, Qing-Guo Huang, 2310.08366 (PRDL)*

*ZCC, Jun Li, Lang Liu, Zhu Yi, 2401.09818 (PRDL)*

- Alternative polarizations

*ZCC, Chen Yuan, Qing-Guo Huang, 2101.06869 (SCPMA)*

*Yu-Mei Wu, ZCC, Qing-Guo Huang, 2108.10518 (ApJ)*

*ZCC, Yu-Mei Wu, Qing-Guo Huang, 2109.00296 (CTP)*

*ZCC, Yu-Mei Wu, Yan-Chen Bi, Qing-Guo Huang, 2310.11238 (PRD)*

- Massive gravity

*Yu-Mei Wu, ZCC, Qing-Guo Huang, 2302.00229 (PRD)*

*Yu-Mei Wu, ZCC, Yan-Chen Bi, Qing-Guo Huang, 2310.07469 (CQG)*

• ...

## Outlook

- IPTA DR3 will contain the timing data from approximately 115 pulsars spanning more than 35 years of observations.
- The search for new physics using the IPTA DR3 is underway . . .

The talk reflects my personal opinions and does not represent the official views of PPTA or IPTA.

Thank you for your  
attention!